Steel and Composite Structures, Vol. 2, No. 6 (2002) 411-428 411
DOI: http://dx.doi.org/10.12989/scs.2002.2.6.411

F. E.-assisted design of the eaves bracket of a cold-formed steel portal frame

J.B.P. Lim†

The Steel Construction Institute

D.A. Nethercot‡

I.C.S.T.M.

(Received July 1 2002, Accepted September 1 2002)

Abstract. Non-linear large-displacement elasto-plastic finite element analyses are used to propose design recommendations for the eaves bracket of a cold-formed steel portal frame. Owing to the thinness of the sheet steel used for the brackets, such a structural design problem is not trivial as the brackets need to be designed against failure through buckling; without availability of the finite element method, expensive laboratory testing would therefore be required. In this paper, the finite element method is firstly used to predict the plastic moment capacity of the eaves bracket. Parametric studies are then used to propose design recommendations for the eaves bracket against two potential buckling modes of failure:

(1) buckling of the stiffened free-edge into one-half sine wave,
(2) local plate buckling of the exposed triangular bracket area.

The results of full-scale laboratory tests on selected geometries of eaves bracket demonstrate that the proposed design recommendations are conservative. The use of the finite element method in this way exploits modern computational techniques for an otherwise difficult structural design problem.

Key words: cold-formed steel; portal frames; eaves joint; finite element analysis.

1. Introduction

The authors have recently described a cold-formed steel portal framing system in which back-to-back cold-formed steel channel-sections were used for the column and rafter members and brackets, bolted between the webs of the channel-sections, were used to form the joints (Lim and Nethercot 2002a, Lim and Nethercot 2002b). The proposed system was designed to both ultimate and serviceability limit states and shown to be capable of spans of up to 18 m.

The general arrangement adopted for the eaves joint of the proposed system is shown in Fig. 1. As can be seen, the most critical component is the back-to-back eaves brackets (Fig. 2). The parameters that will be used to define the geometry of the eaves bracket are shown in Fig. 3.

The eaves brackets are required to sustain a bending moment of the same order as the moment capacity of the back-to-back channel-sections. A method for calculating the plastic moment-capacity

†Formerly, Research Student, University of Nottingham
‡Formerly, Professor, University of Nottingham

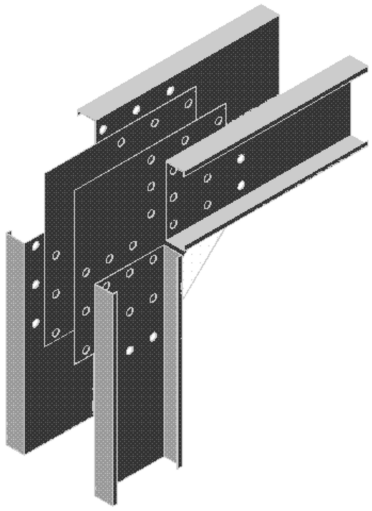

Fig. 1 General arrangement of eaves joint of cold-formed steel portal frame having bolted moment-connections

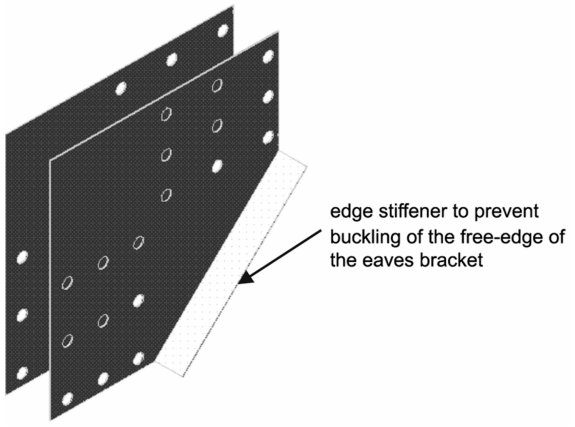

Fig. 2 Details of back-to-back eaves brackets

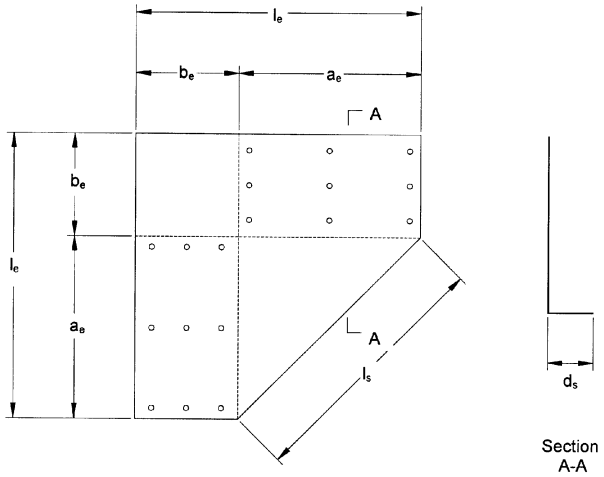

Fig. 3 Diagram showing parameters of eaves bracket

M_p of the eaves brackets is presented herein. However, owing to the thinness of the material used for the brackets, they will need to be designed against failure by buckling. Two potential buckling modes can be identified:

(1) buckling of the stiffened free-edge of the eaves bracket into a one-half sine wave. The stiffener along the free-edge should be designed to prevent this mode of failure by making it sufficiently stiff that it effectively acts as a simply-supported edge to the eaves bracket.

(2) local plate buckling of the exposed triangular area of the eaves bracket. To investigate this mode of failure, plate imperfections are modelled in the eaves bracket and the moment-capacity of the bracket determined. The stiffener along the free-edge is not modelled; instead the free-edge is assumed

to be simply-supported thus idealising the stiffener as a member having zero-axial rigidity and infinite flexural rigidity. With this approach, the plate is designed independently of the stiffener.

In this paper, non-linear large-displacement elasto-plastic finite element analyses are used to provide design recommendations for the design of the eaves brackets against both buckling modes of failure.

Full-scale laboratory tests on selected geometries of eaves bracket are also described; the results of these tests demonstrate that the proposed design recommendations are conservative.

2. Literature review

Unlike the eaves joint of hot-rolled steel portal frames, design recommendations for the eaves joint of cold-formed steel portal frames are not found in any of the codes of practice (BS5950: Part 5 1992, Eurocode 3 1996 and AISI 1996) or design guides (BCSA 1995a, BCSA 1995b) or textbooks (Davies and Brown 1996, Horne and Morris 1981, Woolcock *et al.* 1999, Owens and Cheal 1989, Kulak *et al.* 1987, Hancock 1998, Rhodes 1991) on portal frames, steelwork connections, or cold-formed steel. Moreover, experimental studies reported in the literature on the eaves joint of cold-formed steel portal frames (Baigent and Hancock 1982, Chung and Lau 1999, Kirk 1986), reviewed elsewhere (Lim 2002), have been more concerned with investigating the behaviour of the frame itself. The brackets have therefore all tended to be over-designed, thus ensuring that failure occurred within the column and rafter members of the frame; design recommendations for the brackets were not proposed.

Finite element work on cold-formed steel bolted connections reported in the literature has mainly been concerned with determining the ultimate bearing strength and the initial elongation stiffness of the bolt-holes (Chung and Ip 2000, Lim and Nethercot 2002c, respectively); in both investigations only a lap-joint under double shear was modelled. A finite element investigation on the ultimate strength of the particular failure mode observed for the apex joints of the system under investigation (Lim and Nethercot 2000a), in which moment-capacity was controlled by failure of the actual channel-sections as influenced by the force transfer of the bolt-grouping is presented elsewhere (Lim and Nethercot 2000d).

The main reason for the lack of design recommendations for the eaves bracket of cold-formed steel portal frames has been the relative lack of popularity of cold-formed steel portal frames. Furthermore, the spans where such frames are more competitive than conventional hot-rolled steel portal frames are at the lighter end of the range; for these frames using over-designed eaves brackets has not been regarded as of major concern.

However, the reason for developing the cold-formed steel portal framing system described in Lim and Nethercot (2002a) and Lim and Nethercot (2002b) was to attempt to extend the range of competitive cold-formed steel portal frames. For this reason, the largest cold-formed steel channel-sections that can currently be rolled were used for the column and rafter members. Back-to-back, the moment capacity of the channel-sections was 82.80 kNm.

Table 1 lists the moment-capacity of the members used in the experimental investigations reported in the literature (Baigent and Hancock 1982, Chung and Lau 1999, Kirk 1986) and illustrates that those used in the present study are significantly stronger. However, with the exception of the study by Baigent and Hancock (1982), the thickness of eaves bracket used for connecting the channel-sections used for the proposed system is similar to that used in other investigations. The eaves joint of the proposed system can therefore be expected to be more susceptible to failure through buckling than the joints of the other frames described in the literature. Guidance for the design of the eaves bracket is therefore required.

Table 1 Comparison of main parameters of tests on cold-formed steel bolted moment-connections reported in the literature

Author	Cold-formed steel sections			Brackets		
	M(kNm)	σ_y(N/mm^2)	single/double	l_e(mm)	t(mm)	single/double
Baigent and Hancock (1982)	9.19	320	single	260	12	single
Chung and Lau (1999)	17.88	450	double	460	2.5	double
Kirk (1986)	32.00	280*	double	530	2.4	double
Lim and Nethercot (2002a)	82.80	280*	double	-	3	double

*design yield stress

3. Plastic moment-capacity of eaves bracket

3.1. Preamble

Non-linear large-displacement elasto-plastic finite element analyses will be used to determine the plastic moment-capacity M_p of the eaves bracket. This value represents the upper bound moment-capacity of the eaves bracket and is obtained on the assumption that the bracket has no geometric out-of-plane imperfections, does not buckle and therefore does not require any lateral restraints.

3.2. Details of idealised loading

Fig. 4 shows details of the idealised loading applied to the eaves bracket. As can be seen, the eaves bracket is loaded through the bolt forces of a 3 × 3 bolt-group. It should be noted that, although a 3 × 3 bolt-group of size $(4/5)a_e$ by $(2/3)b_e$ has been used, by St Venant's principle the results obtained should still be applicable to a different array of bolt-group of somewhat similar size.

3.3. Details of finite element mesh

A series of eaves brackets was modelled, having different values of a_e and b_e. For each eaves bracket considered, 16 elements were used along the side BC with the number of elements used along the side

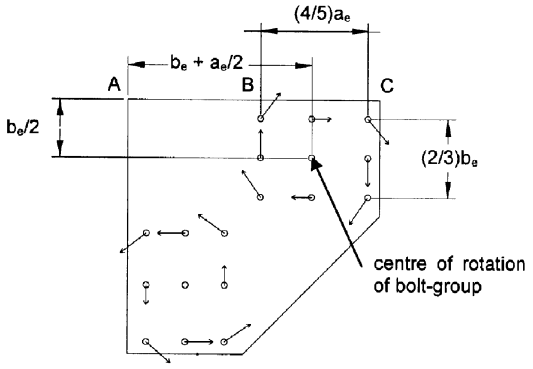

Fig. 4 Details of idealised loading applied to eaves bracket

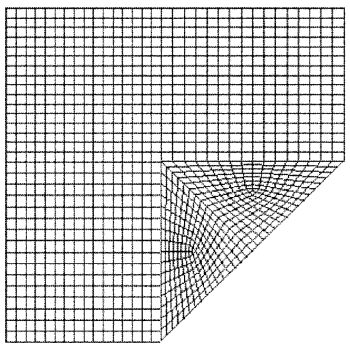

Fig. 5 Details of finite element mesh of eaves bracket

AB chosen to maintain an aspect ratio close to unity for these elements. Fig. 5 shows the finite element mesh of a typical eaves bracket with $b_e/a_e = 0.85$. It can be seen from this figure that 14 elements are used along the side AB.

The general purpose finite element program ABAQUS (Hibbit, Karlsson and Sorensen, Inc. 1995a) is used for the analysis, with the eight-noded thin shell element S8R5 (Hibbit, Karlsson and Sorensen, Inc. 1995b) being used for the eaves bracket.

3.4. Finite element results

The plastic moment-capacity M_p of the eaves bracket was determined from finite element analyses of the eaves bracket. As initial imperfections were not modelled, M_p may be considered as the upper bound to the ultimate moment-capacity M_u of the eaves bracket, which is to be determined in Section 5 by the inclusion of buckling considerations in the finite element model.

From geometric considerations of the eaves bracket, M_p is clearly a function of a_e, b_e/a_e and t as well as σ_y. To determine the relationship, finite element models of the eaves bracket were solved having $a_e = 500$ mm, $b_e/a_e = 0.05$ to 0.9 in increments of 0.05, and $t = 3$ mm. Although the analysis was restricted to this geometry of eaves bracket, it should be noted that, by virtue of dimensional analysis, the results will also be valid for different sizes and thicknesses of bracket. The stress-strain relationship of the material forming the eaves bracket was assumed to be elastic-perfectly-plastic with a yield and ultimate stress of 280 N/mm^2. Fig. 6 shows the variation of M_p against b_e/a_e obtained from the finite element analyses. By curve-fitting the results

$$M_p = \sigma_y a_e^2 t\{0.0675 + 0.4886(b_e/a_e) - 0.1466(b_e/a_e)^2\} \quad (1)$$

for the range

$$0.05 \leq b_e/a_e \leq 0.90$$

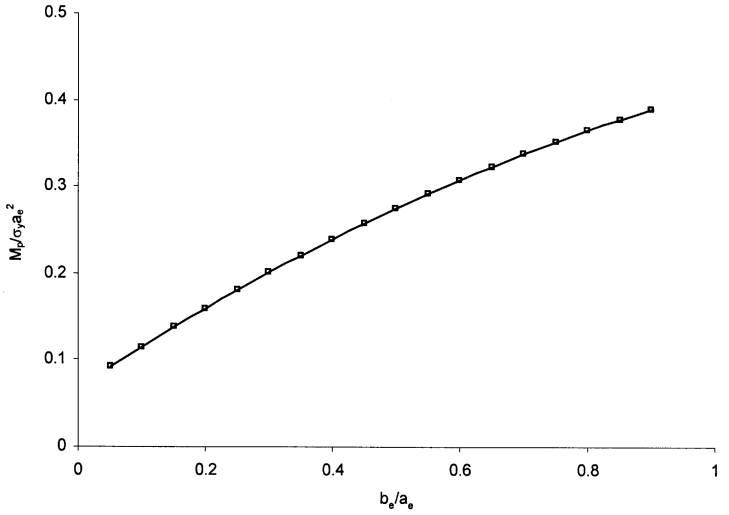

Fig. 6 Variation of plastic moment-capacity M_p of eaves bracket against b_e/a_e

4. Buckling of stiffened free-edge of eaves bracket

4.1. Preamble

The free-edge of the eaves bracket is susceptible to buckling into a one-half sine wave and in order to prevent this mode of failure, a stiffener should be provided along the free-edge (Fig. 2). As can be seen, the stiffener is formed through a fold along the free-edge of the eaves bracket.

While the presence of the stiffener is necessary to prevent buckling of the free-edge, the material cost of the stiffener itself is small and so the depth of the stiffener should ideally be as large as is practically possible. Nevertheless, a simple design rule for the stiffener depth should be provided.

4.2. Details of imperfections

The maximum out-of-plane deviation from straightness of a stiffener formed through a fold is given in BS ENV 1090-2 (1998). This maximum deviation from straightness will be adopted for the magnitude of stiffener imperfection w_s along the free-edge of the eaves bracket (see Fig. 7)

$$w_s = \frac{2.5}{1000} l_s \tag{2}$$

4.3. Depth of stiffener along hypotenuse of triangular plate

Fig. 8 shows a triangular plate loaded through self-equilibrating bending tractions. A design rule for the stiffener depth d_s is required, assuming that the stiffener is formed through a lip along the free-edge of the triangular plate.

Triangular plates of different widths a_t were considered. For each plate under consideration, the stiffener depth d_s was increased until any further increase in d_s results in a negligible increase in the moment capacity of the triangular plate.

Two design rules for d_s are suggested. The first is based on the elastic critical load, determined through elastic critical Eigen-value finite element analyses. The second is based on the results of non-linear large-displacement elasto-plastic finite element analyses, which incorporates both stiffener and local plate imperfections in the finite element model.

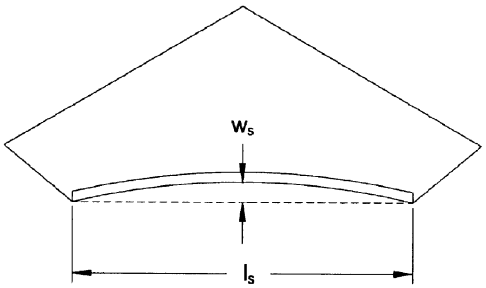

Fig. 7 Details of magnitude of out-of-plane stiffener imperfection

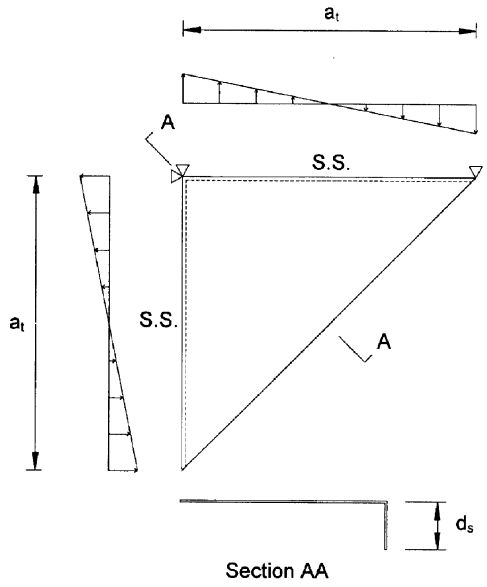

Fig. 8 Details of edge-stiffened triangular plate used in parametric study to determine stiffener depth

4.3.1. Eigen-value finite element analysis

Background to the elastic critical buckling problem of triangular plates is given by Wang and Liew (1994).

The elastic critical buckling moment M_{cr} was first determined for a triangular plate simply-supported along all three sides. This value of M_{cr} is designated as M_{crss}. The required depth of stiffener for the edge-stiffened triangular plate was then defined as the value of d_s that results in the value of M_{cr} for this plate being the same as M_{crss}.

The proposed design rule for d_s is shown in Fig. 9. Curve fitting the results gives

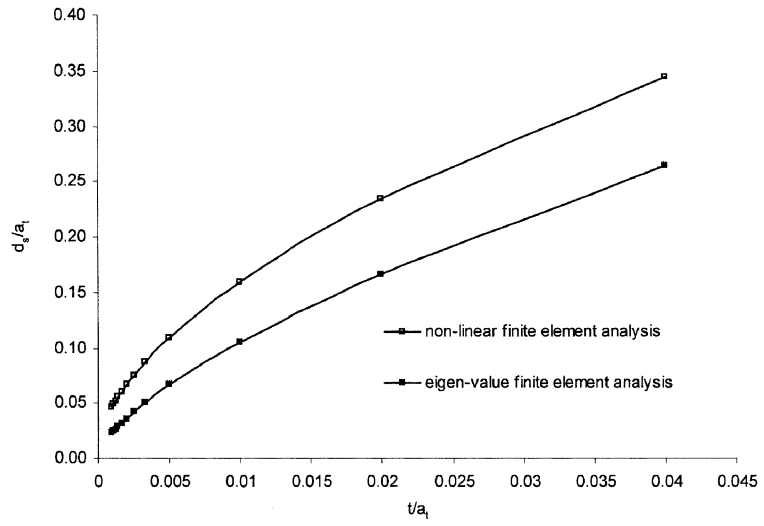

Fig. 9 Design chart for variation of stiffener depth against plate thickness

$$d_s / a_t = 2.26(t/a_t)^{0.67}$$

where

d_s is the depth of the stiffener
a_t is the width of the triangular plate

4.3.2. Non-linear large-displacement elasto-plastic finite element analysis

Adopting standard techniques for stiffener design (Stanway *et al.* 1993), the required depth of stiffener is defined as the value of d_s that allows the plate to carry 95% of the ultimate moment capacity of the triangular plate.

The proposed design rule for d_s is also shown in Fig. 9. Curve fitting the results gives

$$d_s/a_t = 1.95(t/a_t)^{0.543} \tag{3}$$

A more detailed account of the basis for this design rule for the stiffener d_s is available (Lim 2001).

4.3.3. Discussion

Elastic critical Eigen-value analysis is not usually a sufficient basis for design of stiffeners as no account is taken of the reduction in strength caused by imperfections. Nevertheless, such analysis can illustrate the trends in behaviour and is still used in some Codes as the basis for design rules.

On the other hand, non-linear large-displacement elasto-plastic finite element analysis is a sufficient basis for design as the effect of imperfections can be properly taken into account. It is not surprising therefore that the stiffener depth d_s designed on the basis of non-linear finite element analysis is larger than that designed on the basis of elastic critical Eigen-value analysis. For this reason, Eq. (3) will be adopted for the stiffener depth d_s in the remainder of this paper.

4.4. Comparison of load applied to eaves bracket and triangular plate

Fig. 10 compares the type of load applied to the eaves bracket with that applied to the triangular plate. As can be seen, the load applied to the triangular plate is more severe than that applied to the exposed triangular area of the eaves bracket. The design rule for the depth of stiffener of the triangular plate given in Eq. (3) should therefore be conservative when applied to the eaves bracket.

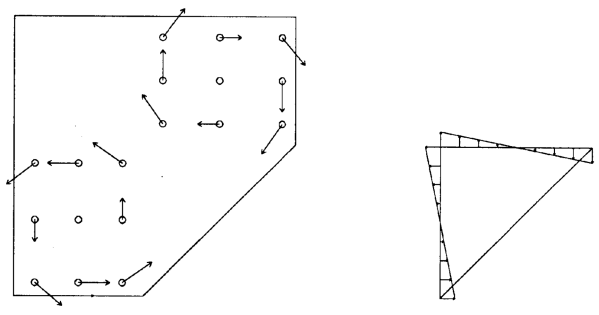

(a) Eaves bracket (b) Triangular plate

Fig. 10 Comparison between load applied to eaves bracket and triangular plate

5. Local plate buckling of exposed triangular area of eaves bracket

5.1. Preamble

In this section, non-linear large-displacement elasto-plastic finite element analyses are used to determine the ultimate moment-capacity M_u of the eaves bracket with imperfections modelled within the exposed triangular area. The stiffener along the free-edge was not modelled; instead the free-edge was assumed to be simply-supported, thus idealising the stiffener as a member having zero-axial rigidity and infinite flexural rigidity.

5.2. Details of idealised lateral restraint and loading

Fig. 11 shows details of the idealised lateral restraint provided to the eaves bracket. The area of the bracket sandwiched between the back-to-back channel-sections in the eaves joint was considered to be fully laterally restrained and, as mentioned previously, the stiffened free-edge of the eaves bracket was assumed to be simply-supported.

The idealised loading applied to the eaves bracket is shown in Fig. 4.

5.3. Details of imperfections

In the absence of actual measurements in the laboratory of the magnitude and contours of imperfections in the plate under consideration, there is no generally accepted standard procedure for selecting the magnitude and contour of initial imperfection for inclusion in finite element models.

Recently, Schafer *et al.* (1996) and Schafer and Pekoz (1998) proposed that the magnitude and contours of imperfection could be treated as random quantities. Using such an approach, it would be possible to properly assess the importance of both these variables. An alternative approach for the contours of imperfections was suggested by Goyet (described in Schafer *et al.* 1996), who proposed that a number of analyses should be performed with the deformed geometry of the previous analysis being used as the initial imperfection in the subsequent analysis. The shape of

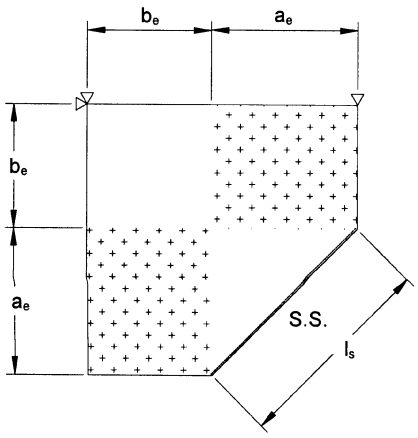

Fig. 11 Details of idealised lateral restraints on eaves bracket used to determine M_u

the initial contours of imperfection used in the first analysis would be obtained from Eigen-value analysis. However, both of these approaches would be too time-consuming for the large number of analyses to be considered.

The magnitude and contours of imperfections adopted for the finite element models to be described are detailed below. As a matter of interest, a limited finite element study showed that the ultimate load was not sensitive to either the magnitude or contours of imperfections. Of more importance is the fact that the imperfections should be modelled.

5.3.1. Magnitude of imperfections

Schafer *et al*. (1996) proposed the following expression for local plate imperfections w_1 based on the thickness of the plate

$$w_1 = 6te^{-2t} \tag{4}$$

where

t is in mm

5.3.2. Shape of imperfections

Initial local plate imperfections were modelled only within the triangular area of the eaves bracket. The shape of these local plate imperfections was obtained from Eigen-value analyses of the eaves bracket.

Fig. 12 shows the typical mode shapes obtained from the Eigen-value analysis. Following standard practice, the first three mode shapes were summed and the resulting shape adopted for the initial imperfection.

5.4. Ultimate in-plane moment-capacity of the eaves bracket

The ultimate in-plane moment-capacity M_u of the eaves bracket with the stiffened-edge assumed to be simply-supported was determined using finite element models of the eaves bracket in which initial local plate imperfections were modelled.

The eight-noded thin shell element S8R5 was again used for the eaves bracket, with six layers through the thickness to allow for the effects of plasticity spread through the thickness of the plate.

The finite element method was used to determine M_u for eaves brackets with a_e = 400 mm to 1200 mm in increments of 200 mm, b_e / a_e = 0.05 to 1 in increments of 0.1, t = 3 mm, and a yield and ultimate

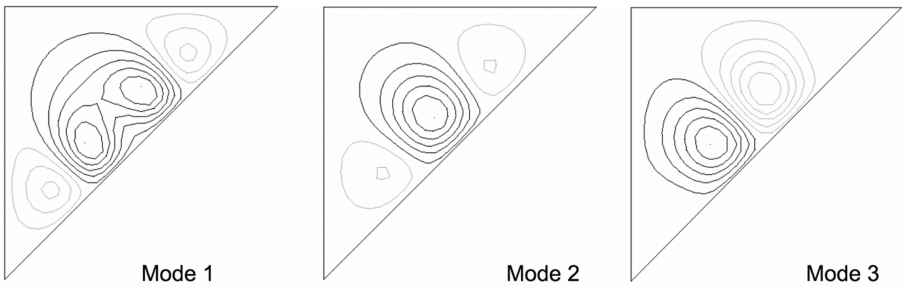

Fig. 12 First three Eigen-mode shapes of exposed triangular area of eaves bracket

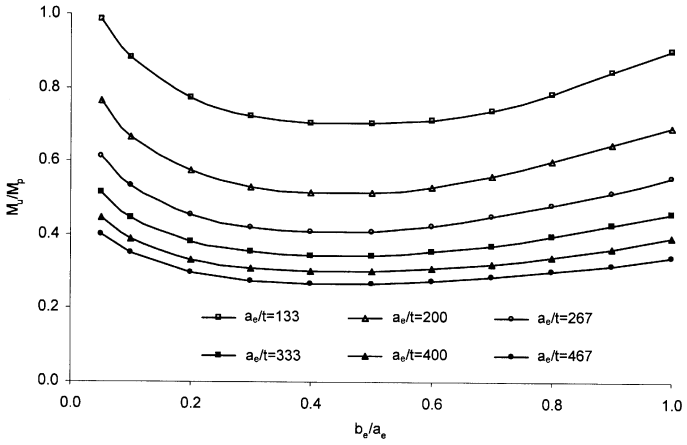

Fig. 13 Variation of M_u against b_e for various values of a_e/t for eaves bracket

stress of 280 N/mm^2.

Fig. 13 shows the variation of M_u against b_e for various values of a_e/t. M_u is non-dimensionalised by M_p to represent the reduction in moment-capacity of the eaves bracket owing to local plate buckling. It can be seen that as the value of the width-to-thickness ratio a_e/t increases (that is, as the plate becomes thinner) the plate becomes more susceptible to local plate buckling and so the ratio M_u/M_p decreases.

6. Application of proposed design rules to some typical eaves brackets

6.1. Preamble

The proposed design rules for the depth of the lip stiffener (Section 4) and the size and thickness of the eaves bracket (Section 5) were developed by considering in isolation the two relevant buckling modes of failure: stiffener buckling and local plate buckling. In this section, the validity of these two rules is tested by applying them to some typical eaves brackets analysed using the finite element method. Both stiffener and local plate imperfections are included in this finite element model of the eaves bracket. The results so obtained are compared against the moment-capacity of the eaves bracket M_u^{des} as given by the design chart of Fig. 13. Table 2 shows the dimensions a_e and b_e of the three eaves

Table 2 Comparison of moment-capacity for some typical eaves brackets

Eaves bracket	a_e(mm)	b_e(mm)	b_e/a_e	d_s[1](mm)	M_p[2](kNm)	M_u^{des}[3](kNm)	M_u[4](kNm)	M_u/M_u^{des}
1	400	200	0.5	54.7	38.0	26.0	31.5	1.21
2	800	320	0.4	75.1	128.7	52.4	65.3	1.25
3	1200	300	0.25	90.4	218.3	69.4	87.1	1.26

[1]Calculated from Eq. (3)
[2]Calculated from Eq. (1)
[3]Determined from Fig.13
[4]Determined from finite element analysis of an actual eaves bracket

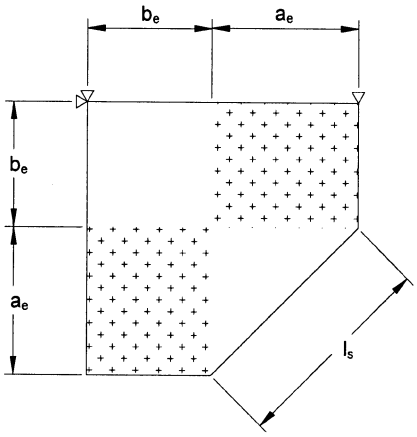

Fig. 14 Details of idealised lateral restraints on eaves bracket used to determine M_u

brackets considered. For each eaves bracket, the depth of stiffener d_s is calculated from Eq. (3).

6.2. Details of finite element model

Unlike the eaves bracket modelled in Section 5, an actual eaves bracket with a lip stiffener is modelled. As before, the value of M_u for the eaves bracket was obtained using non-linear large-displacement elasto-plastic finite element analysis.

Details of the idealised lateral restraint applied to the eaves bracket are shown in Fig. 14. The loading applied to the eaves bracket was the same as for previous idealisations and is shown in Fig. 4. Also, the same finite element mesh was used for the eaves bracket as for previous idealisations (Fig. 5).

The shell element S8R5 used for the eaves bracket was also used for the stiffener. The number of elements used for the depth of the lip stiffener was chosen so as to maintain an aspect ratio close to unity for these elements.

Both stiffener and local plate imperfections were modelled. The magnitude of the stiffener and local plate imperfections were as given in Eq. (2) and Eq. (4), respectively.

6.3. Moment-capacity of eaves bracket

Fig. 15 shows the variation of moment against stiffener deflection for the three eaves brackets under consideration. The dotted line shown in each of the three graphs of Fig. 15 is the value of M_u^{des} as determined from the design chart of Fig. 13 for the relevant size of plate. Table 2 compares the value of M_u^{des} against M_u as determined from the finite element analysis of the actual eaves bracket.

As can be seen from Table 2, the ultimate moment M_u for all three eaves brackets is higher than M_u^{des} by an average of 24%. This result is not unexpected as the axial rigidity of the lip stiffener was ignored when determining M_u^{des}. The results therefore justify the separate treatments for the design of the lip stiffener (against buckling into a one-half sine wave) and the design of the eaves bracket (against local plate buckling in the exposed triangular area) as a conservative simplification.

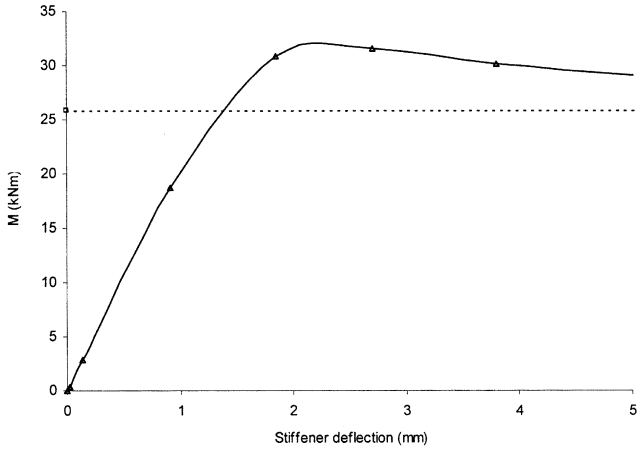

(a) Eaves bracket having a_e = 400mm, b_e = 200mm and d_s = 54.7mm

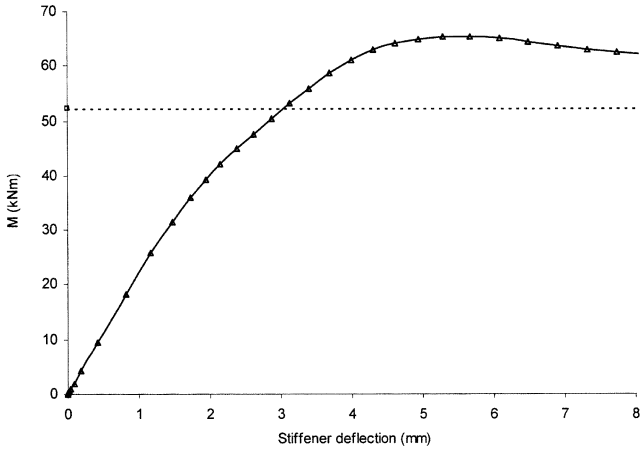

(b) Eaves bracket having a_e = 800mm, b_e = 320mm and d_s = 75.1mm

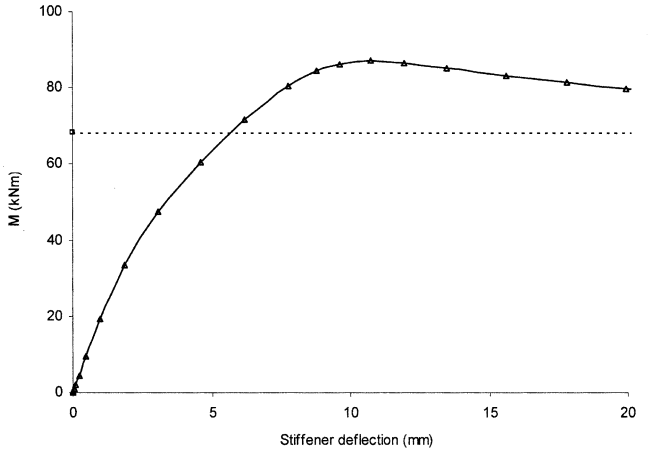

(c) Eaves bracket having a_e = 1200mm, b_e = 300mm and d_s = 90.4mm

Fig. 15 Variation of in-plane moment against stiffener deflection for different sizes of eaves brackets

7. Laboratory tests on eaves joint

7.1. Preamble

Moment-capacity tests were conducted on a series of eaves joints with eaves brackets having values of a_e of 400 mm and 800 mm (Fig. 16). The channel-sections used fixed the value of b_e for the eaves brackets at 340 mm.

The dimensions of the eaves brackets tested are shown in Table 3. As can be seen, four tests were conducted for the eaves brackets having a value of a_e of 400 mm, with each bracket using a different depth of lip stiffener. Only a single test was conducted for the bracket having a value of a_e of 800 mm.

Each of the joints tested only had a single bracket, in order to ensure that the moment-capacity of the brackets would not exceed that of the channel-sections. Clearly, if the moment-capacity of the eaves brackets did exceed that of the channel-sections, then the channel-sections would fail and not the eaves brackets.

7.2. Laboratory test set-up

Details of the points of lateral restraint applied to the eaves joint are shown in Fig. 17. For both sizes of eaves joint, the maximum distance between points of lateral restraint did not exceed the maximum unrestrained distance of 1365 mm that was calculated in accordance with BS5950: Part 5 for lateral-torsional buckling.

Around the eaves bracket only two points of lateral restraint were used. As none of the eaves joints tested failed through lateral-torsional buckling, two points of lateral restraint were therefore sufficient.

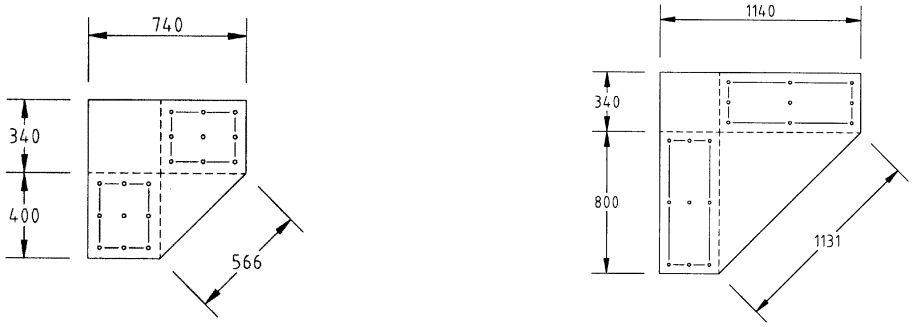

(a) Eaves bracket having a_e = 400mm and b_e = 340mm (b) Eaves bracket having a_e = 800mm and b_e = 340mm

Fig. 16 Dimensions of eaves bracket in laboratory tests

Table 3 Experimental results of tests conducted on eaves joint

Test	a_e(mm)	b_e(mm)	d_s(mm)	t(mm)	σ_y(N/mm^2)	M_u^{exp}(kNm)	$(M_u^{exp})_{norm}$(kNm)
1	400	344	20.4	2.91	207	33	44.6
2	400	352	31.5	2.98	214	40	52.3
3	400	346	46.8	2.96	209	45	60.3
4	400	342	102.6	2.98	213	52	68.9
5	800	346	61.0	2.95	218	66	84.8

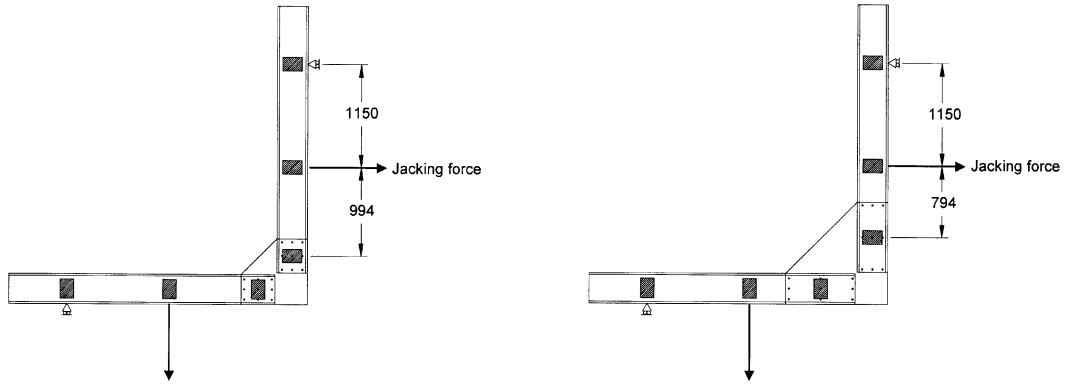

(a) Eaves joint test having a_e = 400mm and b_e = 340mm (b) Eaves joint test having a_e = 800mm and b_e = 340mm

Fig. 17 Details of lateral restraint and loading applied to eaves joint in laboratory tests

7.3. Magnitude of stiffener imperfection

To estimate the stiffener imperfection, a metre rule was placed along the free-edge of the eaves bracket. The straightness of the metre rule had previously been checked by placing its edge on a perfectly flat measuring plane; by eye, no deviation from straightness of the metre rule could be seen. When the metre rule was placed along the free-edge of each eaves bracket, the stiffener imperfection w_s was estimated to be less than 0.5 mm.

With hindsight, a test-rig to measure both the magnitude of stiffener imperfection w_s and local plate imperfection w_1 should have been designed. Such a test-rig would also have enabled the shape of both types of imperfection to be plotted.

7.4. Laboratory test results

The moment-capacity M_u^{exp} obtained from the laboratory tests is also given in Table 3. The observed mode of failure of all tests was buckling of the stiffener.

Three coupons were cut from each eaves bracket, and the material stress-strain properties determined from a tensile test; the average yield stress measured is shown in Table 3. In order that the test results may be compared directly, the value M_u^{exp} recorded for each test is divided by its yield stress and then multiplied by the nominal yield stress of 280 N/mm^2. This value is shown in Table 3 as $(M_u^{exp})_{norm}$.

8. Comparison of laboratory test results against proposed design rules

Table 4 compares the normalised moment-capacity $(M_u^{exp})_{norm}$ to the value of M_u^{des} obtained using the design chart of Fig. 9. It can be seen for the eaves brackets having a value of a_e of 400 mm that an increase in the value of d_s from 20.4 mm to 102.6 mm results in a 54% increase in $(M_u^{exp})_{norm}$. This increase in $(M_u^{exp})_{norm}$ can be attributed to the increased load carried by the stiffener as its size increases. On the other hand, the value of M_u^{des} assumes that the applied load is carried only by the eaves bracket and takes no account of the additional load that can be carried by the stiffener.

Table 4 Comparison of experimental and design rules predicted for eaves joint

Test	d_s(mm)	d_s^1(mm)	d_s/d_s^1	M_p^2(kNm)	$M_u^{des\,3}$(kNm)	$(M_u^{exp})_{norm}$(kNm)	$(M_u^{exp})_{norm}/M_u^{des}$
1	20.4	54.7	0.37	50.7	41.1	44.6	1.09
2	31.5		0.57			52.3	1.27
3	46.8		0.86			60.3	1.47
4	102.6		1.88			68.9	1.68
5	61.0	75.1	0.81	133.7	54.1	84.8	1.57

[1]Calculated from Eq. (3)
[2]Calculated from Eq. (1)
[3]Determined from Fig. 13

Table 4 also compares the depth of the stiffener d_s to the depth recommended by Eq. (1). While the depth of stiffener used in tests in 1, 2 and 3 is less than the depth recommended by Eq. (1), it can be seen that $(M_u^{exp})_{norm}$ is still larger than M_u^{des}. Again, this is attributed to the fact the design rules take no account of the load that can be carried by the stiffener.

9. Some design considerations

It may be of concern that use of the design recommendations will result in brackets substantially larger than necessary. However, the dominant design consideration when determining the size of the brackets is not the ultimate strength of the brackets but the serviceability limit state of acceptable deflections of the frame (Lim and Nethercot 2002a, Lim and Nethercot 2002b). This is because of the rotational flexibility of the proposed joints, the result of the bolt-hole elongation caused when the joints resist a moment load (Lim and Nethercot 2002c). To reduce frame deflections, the size of the bolt-group can be increased. However, since increasing the size of the bolt-group will require a larger bracket, the size of the bracket will therefore be controlled by serviceability considerations of the frame.

The design procedure used in practice will therefore be to first determine the size of the eaves bracket to be used for the joints through considerations of the serviceability requirements of the frame. The design chart of Fig. 9 will then be used to check that back-to-back brackets of the required size can transfer the moment-capacity of the back-to-back channel-sections. Eq. (1) will then be used to determine the depth of stiffener.

The design procedure further justifies the separate treatments for the design of the lip stiffener (against buckling into a one-half sine wave) and the design of the eaves bracket (against local plate buckling in the exposed triangular area).

10. Conclusions

In this paper simple design recommendations have been proposed for what is essentially a complex problem, namely, the behaviour of the eaves bracket in a cold-formed steel portal framing system. Two bucking modes of failure have been identified and treated in isolation:

(1) buckling of the stiffened free-edge of the eaves bracket into a one-half sine wave. A design rule

for the depth of stiffener necessary if it is to provide a simply-supported condition to the edge of the plate was suggested.

(2) local plate buckling of the exposed triangular area of the eaves bracket. A design chart was presented for the ultimate moment capacity (designated as M_u^{des}) (Fig. 13), determined through modelling local plate imperfections within the eaves brackets.

Some typical eaves brackets using the recommended depth of lip stiffeners (Eq. 3) were analysed and the ultimate moment-capacity M_u so obtained compared to M_u^{des}. As the value of M_u^{des} was close (but consistently lower) than M_u, the separate treatments for the design of the lip stiffener against stiffener buckling and that of the eaves bracket against local plate buckling have been justified and the value of M_u^{des} can be used conservatively in the design of actual eaves brackets.

Laboratory tests were conducted and it was demonstrated that M_u^{des} determined from the proposed design rules provided safe predictions of M_u^{exp}.

The complete study demonstrates how modern numerical analysis techniques of the sort that are now readily available to the research community may be used to develop design rules for complex structural components. Such an approach greatly reduces the need for expensive and time consuming laboratory study, whilst maintaining realistic and safe coverage of all important structural issues.

Acknowledgements

The authors would like to acknowledge the technical support provided by Messrs Gerry Barnes, Michael Bettison, Gary Hayes, Bal Loyla, Geoffrey Mitchell, Melvyn Ridal, Nigel Rook and Brian Whitehouse of the Heavy Structures Laboratory at the University of Nottingham where the experimental work described herein was conducted. The work was undertaken in association with Ayrshire Metal Products as a "Partners in Technology" project with financial support from the DETR.

References

AISI (1996), *Specification for The Design of Cold-Formed Steel Structural Members.* American Iron and Steel Institute, Washington.

Baigent, A.H. and Hancock, G.J. (1982), "The behaviour of portal frames composed of cold-formed members", *Thin-Walled Structures - Recent technical advances and trends in design, research and construction*, Elsevier Applied Science, Oxford, p209.

BS5950: Part 5 (1992), *Code of Practice for Design of Cold-Formed Sections*, British Standards Institution, London.

Chung, K.F. and Ip, K.H. (2000), "Finite element modeling of bolted connections between cold-formed steel strips and hot-rolled steel plates under static shear loading", *Engng Struct*, **22**, 1271.

Chung, K.F. and Lau, L. (1999), "Experimental investigation on bolted moment connections among cold-formed steel members", *Engng Struct*, **21**, 898.

Davies, J.M. and Brown, B.A. (1996), *Plastic Design to BS 5950*, Ascot, The Steel Construction Institute, Blackwell Scientific Publishers.

Eurocode 3 (1996), *Design of Steel Structures: Part 1.3 - General rules and rules for buildings*, Committee European de Normalisation, Brussels.

Hancock, G.J. (1998), *Design of Cold-Formed Steel Structures*, Australian Institute of Steel Construction, 3rd ed..

Hibbit, Karlsson and Sorensen, Inc. (1995a), *ABAQUS Theory Manual*, Hibbitt, Karlsson and Sorensen, Inc.

Hibbit, Karlsson and Sorensen, Inc. (1995b), *Element selection in ABAQUS/Standard*, ABAQUS Lecture Notes Series, Hibbitt, Karlsson and Sorensen, Inc.

Horne, M.R. and Morris, L.J. (1981), *Plastic Design of Low-Rise Frames*, Constrado monograph, Granada Publishing.

Kirk, P. (1986), "Design of a cold-formed section portal frame building system", *Proc. 8th International Speciality Conference on Cold-formed Steel Structures*, St. Louis, University of Missouri-Rolla, 1986, p295.
Kulak, G.C, Fisher, J.W. and Struik, J.H.A. (1987), *Guide to Design Criteria for Bolted and Riveted Joints*, 2nd ed., John Wiley and Sons, New York.
Lim, J.B.P. (2001), "Joint effects in cold-formed steel portal frames", University of Nottingham, PhD thesis.
Lim, J.B.P. and Nethercot, D.A. (2002a), "Design and development of a general cold-formed steel portal framing system", *The Structural Engineer*, **80**(21), 2002, 31.
Lim, J.B.P. and Nethercot, D.A. (2002b), "Serviceability design of a cold-formed steel portal frame having semi-rigid joints", *to be submitted.*
Lim, J.B.P. and Nethercot, D.A. (2002c), "Stiffness prediction for bolted moment-connections between cold-formed steel members", *to be submitted.*
Lim, J.B.P. and Nethercot, D.A. (2002d), "Ultimate strength of bolted moment-connections between cold-formed steel members", *to be submitted.*
Owens, G.W. and Cheal, B.D. (1989), *Structural Steelwork Connections*, Butterworth, London.
Rhodes, J. (1991): *Design of Cold-Formed Steel Members*, Elsevier Applied Science, Oxford.
Schafer, B.W., Grigoriu, M., Pekoz, T. (1996), "A probabilistic examination of the ultimate strength of cold-formed steel elements", *Proc. 13th International Speciality Conference on Cold-Formed Steel Structures*, St Louis, University of Missouri-Rolla.
Schafer, B.W., Pekoz, T. (1998), "Computation modeling of cold-formed steel: characterizing geometric imperfections and residual stresses", *Thin-Walled Structures,* **47**, 193.
SCI/BCSA (1995a), *Joints in Steel Construction: Simple Connections*, SCI/BCSA.
SCI/BCSA (1995b), *Joints in Steel Construction: Moment Connections*, SCI/BCSA.
Stanway, G.S., Chapman, J.C. and Dowling, P.J. (1993), "Behaviour of a web plate in shear with an intermediate stiffener", *Proc. Instn Civ. Engrs Structs Bldgs*, **99**, 327.
Wang, C.M. and Liew, K.M. (1994), "Buckling of triangular plates under uniform compression", *Engng Struct.*, **16**, 43.
Woolcock, S.T., Kitipornchai, S., Bradford, M.A. (1999), *Limit State Design of Portal Frame Buildings,* 3rd ed., Australian Institute of Steel Construction, Sydney.

Notation

a_e : width of triangular area of eaves bracket
a_t : width of triangular plate
b_e : edge width of eaves bracket
d_s : depth of stiffener
l_a : half-length of apex bracket
l_e : length of eaves bracket
l_s : length of stiffener
M_p : plastic moment-capacity of bracket
M_u : ultimate moment-capacity of bracket
M_u^{ana} : M_u as determined from finite element analysis (numerical test)
M_u^{des} : M_u of bracket as determined from proposed design rules
M_u^{exp} : M_u as determined from experimental test
t : thickness of plate
w_l : amplitude of initial out-of-plane local plate imperfection
w_s : amplitude of initial out-of-plane stiffener imperfection
σ_u : ultimate stress
σ_y : yield stress

SC